Experimental Measurements of Low-Frequency Intermolecular Host−Guest Dynamics

Alexander P. Sukharevsky, Ian Read, Brian Linton,† Andrew D. Hamilton,† and David H. Waldeck*

Department of Chemistry, University of Pittsburgh, Pittsburgh, Pennsylvania 15260

Received: March 9, 1998; In Final Form: April 21, 1998

A direct temporal measurement of the internal motion of a host−guest bimolecular complex is reported. Time-resolved polarization spectroscopy is used to monitor the motion of a guest chromophore, anthracene-1,3-dicarboxylate, bound to a bis(guanidinium) host molecule through a combination of hydrogen bonding and electrostatic forces. The dynamics of the bound chromophore is well described by an overdamped oscillator model. Through simple modeling, it is possible to estimate the frequency of the host−guest potential and the range of the guest chromophore's angular displacement.

I. Introduction

Intermolecular interactions and complexation play an important role in many chemical and biological processes. A bimolecular complex contains a receptor unit(s) that binds a guest (or substrate) molecule. The experimental characterization of host−guest systems is typically accomplished by measuring the association constant K_a and determining the thermodynamic parameters ΔH and ΔS to provide a *static* binding picture. Although such studies have led to a useful understanding of the importance of the structural features and interactions which can control binding, they do not address important *dynamical* questions. For example, "what is the rate of dissociation of the complex", or "how rigid is the complex"? Obtaining answers to these questions and predicting and controlling the dynamics of a complex is necessary for the rational design of artificial enzymes and other molecular scale machines.

The importance of the dynamical issues in biological systems is apparent in the extensive literature focusing on the motion of side groups in proteins and artificial probes bound to proteins and other biomolecules. Yet the development of structure−function relationships and a detailed evaluation of molecular dynamics results are not available. The work described below is an initial step toward the long-term goal of investigating the orientational dynamics of synthetic host−guest systems in which the properties of the complex can be chemically tuned. The primary methods which have been used to investigate orientational dynamics in biological systems are NMR[1] and fluorescence depolarization.[2] The fluorescence depolarization method provides a direct temporal measurement of the chromophore's orientational relaxation, but only for the electronically excited state. The study described below is a direct temporal measurement of the orientational motion in the ground electronic state of a chromophore that is bound to a receptor.

This study addresses the flexibility of intermolecular complexes, presenting experimental results on the orientational dynamics of a guest chromophore bound to a host molecule through a combination of hydrogen-bonding and electrostatic forces. The structures in Figure 1 show both guest and host molecules in a geometry that illustrates the two-point binding

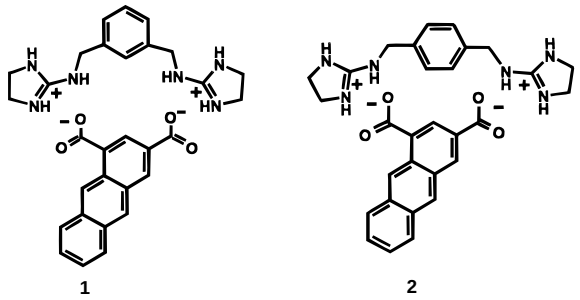

Figure 1. Molecular structures of the two complexes. The guest chromophore was prepared as the anthracene-1,3-dicarboxylate bis-(tetrabutylammonium) salt.

envisioned for these systems. The guest molecule is anthracene-1,3-dicarboxylate (ADC) and the host molecules are two bis-guanidinium receptors with different site geometries. The two complexes shown in Figure 1 bind with an association constant in excess of 10^5 M^{-1}, as determined by fluorimetric and calorimetric binding curves. The binding of carboxylates with guanidiniums in polar solvents has been studied in detail.[3,4] These studies indicate that the carboxylate groups interact with the guanidinium moieties. The investigation of artificial systems of this sort is aided by the direct synthetic control of the system parameters and should allow for the identification of structure−function relationships.

The relative motion of the host and guest molecules is followed using femtosecond time-resolved optically heterodyned polarization spectroscopy (OHPS).[5] This technique probes relaxation of an absorption dichroism that is induced in the sample with a linearly polarized, ultrafast laser pulse. The wavelength of the laser is tuned to an electronic absorption of the anthracene chromophore, and hence the transition dipole moment of the anthracene acts as a vector defining the molecule's orientation in space. A vertically polarized femtosecond laser pulse (the pump pulse) excites the sample and creates a spatial anisotropy in the distribution of ground state anthracene orientations. A second laser pulse (the probe pulse) whose polarization is oriented 45° from the first pulse probes this anisotropy in the molecular orientations. By changing the relative arrival time of the pump and probe pulses in the sample, the decay of the pump-induced anisotropy can be obtained. The OHPS method uses a special detection scheme that is able to

† Current address: Department of Chemistry, Yale University, New Haven, CT 06520.

S1089-5647(98)01417-5 CCC: $15.00
Published on Web 06/05/1998

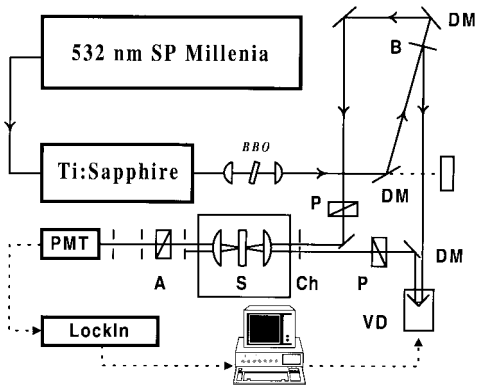

Figure 2. A schematic diagram of the femtosecond polarization spectrometer: P, polarizers; A, analyzer polarizer; DM, dichroic mirror; B, beam splitter; Ch, optical chopper; S, sample; VD, variable delay.

restrict the signal to only those chromophores that are resonant with the probe pulse's wavelength. For the anthracene system the OHPS signal is well described by the expression

$$\text{signal} \propto r(t)\, K(t) \tag{1}$$

where $r(t)$ is the anisotropy and $K(t)$ is the ground state population recovery.[5] For the system studied here, the population recovery $K(t)$ is much slower than the anisotropy, and the signal is well approximated as $r(t)$.

The OHPS experiment selectively probes the orientational motion of the anthracene chromophore in its ground electronic state. For the case of the ADC free in solution (no host is present), this method measures the rotational relaxation of the chromophore (vide infra). When the ADC is bound to the guanidinium host its rotational motion is restricted. In this case the relaxation is characterized by a low-frequency bending vibration of the chromophore relative to the complex and the overall rotation of the complex. This method is capable of selectively probing this torsional relaxation of the ADC chromophore, to the exclusion of other low-frequency vibrational motions present in the system.

The time-resolved data for the relaxation characteristics of these host−guest complexes is presented below. The relaxation data for free ADC in dry DMSO is compared to that for the ADC bound in the complex, demonstrating a change in the characteristic decay law from a single exponential for the ADC in free solution to a nonexponential relaxation for ADC bound to the host. On a qualitative level, the orientational dynamics of ADC in the complex can be well described as a damped oscillator. Using a simple harmonic model, it is possible to estimate the frequency of the host−guest torsional potential and the mean square angular fluctuation of the guest chromophore.

The manuscript is divided into six sections. Section II describes the femtosecond OHPS spectrometer that was constructed for these studies and other experimental details. Section III discusses the characterization of the host−guest complexes, namely their spectra and binding curves. Section IV presents the anisotropy measurements for the chromophore in free solution and bound to the receptor. Section V outlines three approaches to modeling the relaxation in these systems. Section VI is the conclusion.

II. Experimental Section

OHPS Spectrometer. A pump−probe spectrometer with a femtosecond laser source was constructed to perform these experiments (see Figure 2). The design of the Ti:sapphire laser is similar to the design of Cerullo and co-workers.[6] The hard aperture in their design was removed in order to operate the oscillator at higher average output power, at the expense of self-starting. The cavity has two arms of approximately equal length (83 cm). A four mirror resonator with an additional fold mirror (ultrafast CVI HR) is pumped by 4 W of 532 nm radiation that is obtained from a diode-pumped solid state (DPSS) laser (Spectra-Physics Millenia). The Ti:sapphire crystal is 10 mm in length (Atramet, 0.09% doped). Daily operating conditions gave ∼700 mW average power with stable 50−80 fs pulses at 800 nm. The fundamental was doubled to 400 nm in a 0.5 mm type I BBO crystal (Skytek). This arrangement yielded 40−60 mW of average power.

The experimental arrangement used for the OHPS measurements in these experiments is similar to earlier designs.[5] The 400 nm output from the laser source was sent into a Michelson interferometer through a 10% beam splitter. The fixed length arm of the interferometer was the pump, and the variable length arm of the interferometer was the probe. The relative arrival time of the pump and probe pulses in the sample was controlled using a translation stage with 1 μm resolution (Klinger). Glan-Laser polarizers (Karl Lambrecht Corp.) with an extinction ratio of $\leq 10^{-6}$ were used to set the polarization of the light pulses. The probe beam polarization was oriented at 45° with respect to the pump beam. The analyzer polarizer (A) was also a Glan-Laser polarizer. Two optical pulses were collinear and displaced 1 in. apart as they entered a 20 cm focus quartz lens that focused them onto the sample. A standard dye laser nozzle (Coherent Inc.) was used to form a liquid jet that was approximately 0.5 mm thick and 3 mm wide. A recollimating lens collected the probe beam after the sample and imaged it on the analyzer polarizer. The sample jet and assembly was enclosed in a glovebag to isolate the sample from the room air and control the water content in the solvent. The glovebag was purged with dry, high-purity nitrogen gas. The analyzer polarizer was positioned with its transmission axis 1° from being crossed with the input probe polarizer. This allows some of the unmodulated probe light (the reference or E_{LO}) to leak through the analyzer. In addition, the signal field (E_{signal}) which is generated by the perturbation induced by the pump pulse leaks through the analyzer polarizer. The interference between E_{LO} and E_{signal} heterodynes the signal field on the detector (PMT, Hamamatsu R1527); see ref 5 for more details. Fluorescence from the sample is eliminated at the detector by an interference filter. The scattered laser light is minimized by three spatial apertures. The pump and the probe beams are chopped at two different frequencies ω_1 and ω_2 by a mechanical chopper (SRS) prior to entering the sample. A zero background signal is detected with a lock-in amplifier (EG&G model 5302) tuned to the difference frequency $\omega_{diff} = \omega_1 - \omega_2$. The signal was processed using a personal computer that runs the ASYST operating environment. The collected decay curves were fit to a functional form using the Axum software package.

Sample Preparation. The ADC chromophore was synthesized from anthraquinone-1,3-dicarboxylic acid which was prepared according to literature methods.[7,8] Benzoyl chloride was added to mesitylene in the presence of aluminum chloride. The crude product was purified by vacuum distillation to yield the corresponding benzophenone. Oxidation of the methyl groups was carried out by the addition of concentrated nitric acid and heating of the solution for 5 days at 180 °C. The benzophenone-1,3,5-tricarboxylic acid was then purified by solvent extraction. Anthraquinone-1,3-dicarboxylic acid was prepared by acid-catalyzed ring closure and the crude product was purified by extraction with ether. The anthracene derivative

was prepared by Zn/NH_4OH reduction of the anthraquinone. ADC was purified by acid-catalyzed esterification in methanol to form the dimethyl ester. The diester was then purified by chromatography (silica gel, 1:1 CH_2Cl_2:hexanes), and the diacid was recovered by reflux of 1 M NaOH in methanol, followed by solvent extraction. The tetrabutylammonium salt was prepared by stoichiometric addition of tetrabutylammonium hydroxide to an aqueous solution of the diacid. The water was then removed by lyophilization. The product was characterized by NMR and GC-MS. The purity of the diester was determined to be 99.6% by GC. The melting point of the diester is 147−149 °C.

DMSO was purchased from J. T. Baker and dried using 200−400 mesh molecular sieves.

Details of the preparation of the host molecules **1** and **2** are reported elsewhere.[4] Host **1** was prepared by adding 2-mercaptodihydroimidazole to a solution of methyl iodide in methanol and refluxing for 6 h. After the reaction mixture was allowed to cool, methanol was removed until the mixture became dark red. Diethyl ether was then added to the reaction mixture and the hydroiodide salt precipitate was collected by suction filtration. The salt was then added to a solution of m-xylylenediamine in THF and refluxed until the release of methanethiol was complete. The precipitate **1** was collected by filtration. A similar procedure was used to prepare **2**.

Characterization of Binding. The binding affinity was determined by titration curves that were measured both calorimetrically and by fluorescence. The fluorescence method used an SLM 8000 fluorimeter. The sample was excited at 390 nm and the fluorescence was monitored at 450 nm. The fluorescence yield of the complex is higher than that of the free molecule. The calorimetric method used an isothermal titration calorimeter (ITC) from Microcal Inc. The calorimetric method provides both the association constant through a titration curve and the enthalpy of association directly.

III. Characterization of the Complexes

Spectra. Figure 3A presents the absorption spectra in DMSO solvent for ADC, its complexes with the host molecules, and the host molecule **1**. The absorption spectrum for the ADC shows the characteristic vibronic structure of the anthracene chromophore. The spectrum is slightly red-shifted from that of anthracene because of the substitution. The spectra for the complexes appear to be very similar to that of the dicarboxylate. A small blue shift of less than 3 nm is evident, however. In contrast to these spectra, the host molecule **1** shows no absorption at 400 nm (the curve shown in the figure has been amplified 100 times). These spectra demonstrate that the time-resolved experiments performed at 400 nm probe the absorbance of the anthracene chromophore.

Figure 3B presents the excitation spectra (measured while monitoring the fluorescence at 450 nm) and the fluorescence spectra of ADC and its complexes with **1** and **2**. These spectra demonstrate that the fluorescence band has the characteristic vibronic structure of the anthracene chromophore. Although unusual photophysics occurs for 9-anthracenecarboxylic acid in some solvents[9] and dimer formation of anthracene carboxylic acids[10] has been reported, these processes have been associated with broad emission bands that are Stokes-shifted from the absorption. These data show that the emission band is well-defined and the Stokes shift is small, and hence such processes are not relevant to the 1,3-anthracenedicarboxylate in dry DMSO that is studied here. Lastly, these spectra demonstrate that the 400 nm probe wavelength should not be affected significantly by stimulated emission from the excited state.[5]

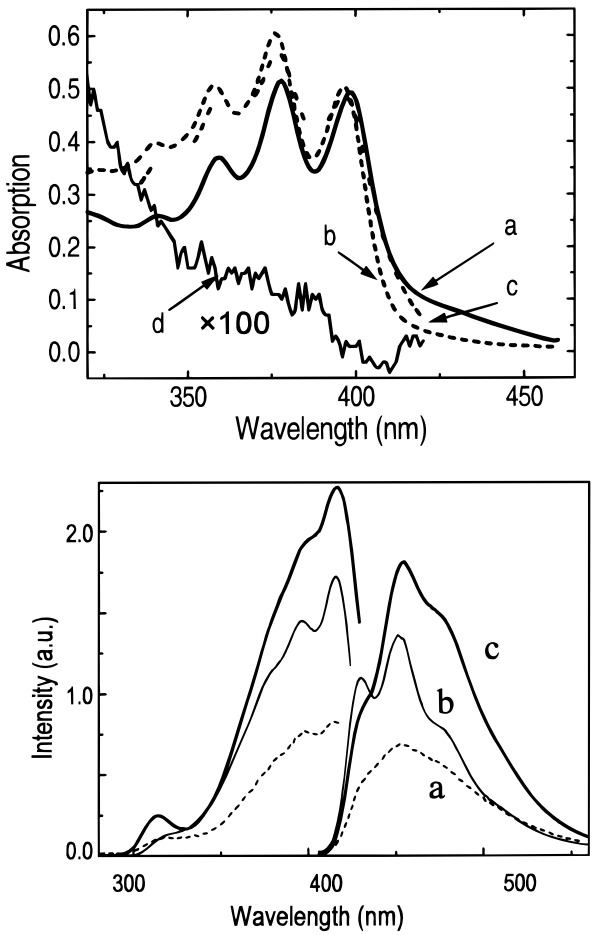

Figure 3. (A, top) Absorption spectra for ADC: a, ADC in DMSO; b, ADC:**2** complex; and c, ADC:**1** complex. The absorption spectrum of **1** in DMSO is the spectrum d, and it has been magnified 100 times over that for ADC. (B, bottom) Excitation and fluorescence profiles for ADC: a, free chromophore (×100 magnification); b, ADC:**2** complex; c, ADC:**1** complex. Excitation wavelength was 390 nm and emission wavelength was 450 nm.

Binding Curves (Calorimetric and Fluorescence). The two artificial receptors (bis(guanidinium) host molecules) chosen for this study (Figure 1, **1** and **2**) exhibit strong electrostatic and hydrogen bonding for oxyanion guests in polar solvents.[4] The association constants for the hosts **1** and **2** with ADC as a guest were determined using two types of titration curves.

Figure 4A shows the fluorimetric titration curves for ADC with **1** and **2** in dry DMSO. In these studies the concentration of the ADC guest was 10^{-4} M or less. The data were fit to the equilibrium given by

$$H + G \rightleftharpoons HG$$

The association constant obtained was in excess of 5×10^5 M^{-1}. Consideration of a second equilibrium in which one guest molecule binds to two host molecules provides a similar binding constant for the 1:1 binding and about 100 M^{-2} for the 1:2 binding. The quality of the fits to the multiple equilibria is not significantly better than that for the 1:1 equilibrium which is shown in the Figure 4A. Because the binding of ADC with **1** and **2** is so strong, it is difficult to precisely determine the value of the binding constant. For this reason the fluorescence data are interpreted as setting a lower limit of 10^5 M^{-1} on the binding constant.

Using the isothermal titration calorimetric method,[11] association constants for both complexes were determined to exceed

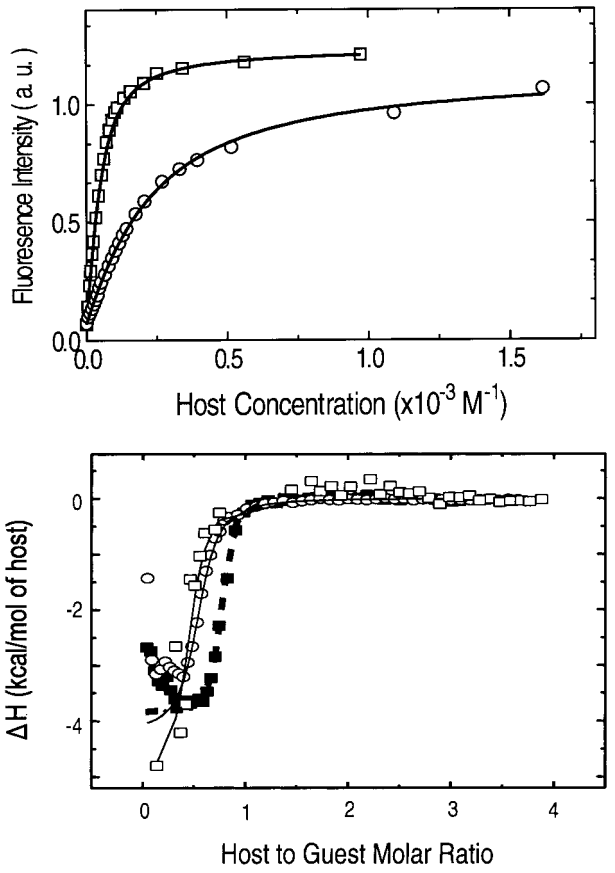

Figure 4. (A, top) Fluorescence binding titrations for ADC/guanidinium complexes. Open squares are ADC:**2** data and circles are ADC:**1** data. Guest concentration was 10^{-3} M. (B, bottom) Calorimetric binding curves are shown for the host−guest complexes. Circles represent the data for ADC:**1** and squares represent the data for ADC:**2**. The filled symbols correspond to a tetraphenylborate counterion, and the open symbols correspond to an iodide counterion. The curves represent fits to the data (solid curves are the iodide salt and dashed curve is the tetraphenylborate salt).

10^5 M^{-1} (see Table 1) in dry DMSO. The binding curves for the host−guest systems are shown in Figure 4B. These data illustrate that when the guest concentration exceeds the host concentration, higher order aggregates (e.g., 2:1) are formed. This aggregation causes the features at low host:guest molar ratio where the enthalpy appears to drop.[4c] As the host concentration increases and exceeds that of the guest, 1:1 binding dominates. The smooth manner in which the measured enthalpy approaches the asymptote indicates that the binding stoichiometry is predominately 1:1, or that the 1:2 binding is isenthalpic. When 1:2 binding is significant, a "hump" appears in the titration curve; i.e., the enthalpy overshoots the asymptote.[4c] All of the spectroscopic studies were performed with a large excess of host molecule so that the concentration of free guest in solution never exceeded 1%. As with the fluorescence data, the binding is very strong and the titration curve is not very sensitive to binding constants in excess of 10^5 M^{-1}. Hence the association constants reported in Table 1 are interpreted as a lower bound on the actual association constant.

The calorimetric method also directly measures the enthalpy of binding for these systems. These values are reported in Table 1. The binding enthalpy is clearly exothermic and significantly larger than kT. The enthalpy of binding has contributions from the solvation energies of the other ions and the salt's lattice energy. This effect is evident from a comparison of the iodide and tetraphenylborate salts of **2**. In the approximation that the lattice energies for the iodide salts of **1** and **2** are the same, these contributions should cancel. A comparison of the data on the iodide salts indicates that the interaction of ADC with **2** is stronger than with **1**. The enthalpy of binding for **2** is 20% stronger than for **1**. Given the similar nature of the guest molecule this difference must reflect changes in the solvation of the hosts and their different abilities to bind the guest.

The conclusions to be drawn from these binding data are 3-fold. First, the binding is strong, in excess of 10^5 M^{-1}. When the host compound is present in 10-fold excess, less than 0.1% of the ADC molecules are uncomplexed in solution. Second, the fits to the fluorescence and calorimetry titration data for 1:1 equilibria indicate that the presence of 1:2 binding at high excess of host concentration is weak, compared to the 1:1 binding. Third, the change in geometrical arrangement of the host binding sites from 1,3- (in **1**) to 1,4-substitution (in **2**) about the xylylene spacer changes the enthalpy of association.

IV. Anisotropy Measurements

The optically heterodyned polarization spectroscopy method measures the orientational anisotropy of the anthracene chromophore. The orientational relaxation of the unbound ADC in DMSO solution should be well described by rotational diffusion. The anisotropy decay of the bound chromophore may reflect contributions from the overall relaxation of the complex as well as internal torsional relaxation. First, the relaxation of ADC in free solution is discussed. Second, the relaxation of ADC within the host−guest complex is discussed.

Rotational Relaxation of Anthracenes. The anisotropy decays of ADC, 9-anthroic acid, and 2-anthroic acid were investigated in DMSO solution. The results reported below are in reasonable agreement with those found for the rotational relaxation of other anthracenes (see Table 2). The anisotropy decay for ADC is shown in Figure 5. This transient fits well to a single-exponential decay law with a lifetime of 30 ps. The error in the relaxation time is determined to be ±3 ps from the measurement of 10 decay curves. Other substitution patterns and substituents of the anthracene (see Table 2) have also been measured. It is apparent from the relaxation times reported for the anthracenecarboxylate and -carboxylic acids in DMSO (see Table 2) that the relaxation time does not depend strongly on the substitution pattern. This general observation is consistent

TABLE 1: Binding Constants, Enthalpies, and Experimental Decay Constants for Anthracene-1,3-dicarboxylate (ADC) and Its Complexes with 1 and 2 in DMSO at 303K[a]

	K_a (10^5 M^{-1})	ΔH (kcal/mol)	τ_1 (ps)	τ_2 (ps)	long
ADC			33 ± 4		
ADC/**1** iodide salt	3.5 ± 0.2	−4.2 ± 0.1	26 ± 15	401 ± 76	0.74 ± 0.18
ADC/**2** iodide salt	5.1 ± 5	−5.2 ± 0.6			
ADC/**2** TPB salt	18 ± 2	−3.9 ± 0.1	14 ± 8	356 ± 22	0.86 ± 0.05

[a] ADC is anthracene-1,3-dicarboxylate bis(tetrabutylammonium) salt. The errors given for K_a and ΔH represent the variance obtained from a fit to the titration data. The error reported for the decay times and the amplitude of the long component (long) represent two standard deviations from an average of six data sets.

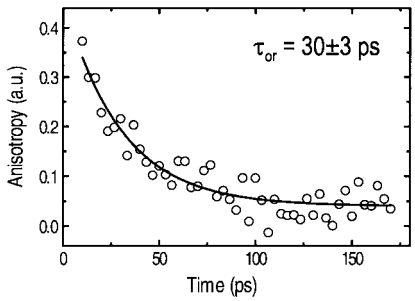

Figure 5. Anisotropy decay for ADC in DMSO at 24 °C. Solid line is a best fit to a single-exponential decay.

TABLE 2: Measured Anisotropy Decay Times for Different Substituted Anthracenes in DMSO

solute	τ (ps)	ref
9,10-dichloranthracene	26	12
9,10-dimethylanthracene	26	12
9-methyl-10-chloroanthracene	27	12
9-chloro-10-cyanoanthracene	35	12
9-methyl-10-cyanoanthracene	44	12
9-anthroic acid	30−40	this study
2-anthroic acid	35	this study
anthracene-1,3-dicarboxylate	30	this study

with a model in which the anthracenes are approximated as an oblate ellipsoid where the unique axis is perpendicular to the plane of the molecule and the molecule's transition dipole moment lies in the molecular plane.[12,13]

The proper modeling of the frictional coupling between a solute and solvent remains an open question. The traditional model of the frictional coupling considers the solvent to be a continuous medium that is characterized by its bulk shear viscosity and treats the solute as a smooth ellipsoid moving through the viscous fluid. Two boundary conditions are commonly used to characterize the coupling between the continuum solute and the solvent. First, the stick boundary condition assumes the relative velocity of the solute and solvent at their boundary to be zero, and hence the first layer of solvent moves with the solute. Second, the slip boundary condition assumes that the tangential component of the relative solute−solvent velocity is infinite; that is, the solute slips past the solvent. More recently, other contributions to the frictional coupling have been included to describe measured relaxation times and diffusion coefficients. One important contribution to the total frictional coupling is dielectric friction[14] which has been discussed by a variety of workers. In some approximations, it is possible to incorporate the dielectric friction into an effective boundary condition in a hydrodynamic or electrohydrodynamic treatment. Other contributions to the friction have also been proposed; most of these may be classified as models which incorporate some sort of solvent attachment or use the concept of a hydrodynamic volume.[15,16]

The relaxation time of ADC in DMSO is consistent with the predictions of a hydrodynamic model with a slip boundary condition. In the hydrodynamic analysis it is necessary to model the solutes volume and its axial radii. The axial radii for ADC was estimated from standard bond lengths and van der Waals increments.[17] The axial radii ADC were taken to be 2:4:6 Å and its volume was taken to be 210 Å^3. A Hartree−Fock calculation indicates that the transition dipole moment for ADC lies in the plane of the ring system and is oriented at 68° from the long axis. Although the rotational relaxation is predicted to be a sum of exponentials, the decay constants of the significant exponential terms are very similar such that the decay is well described by a single exponential.[12] For the stick

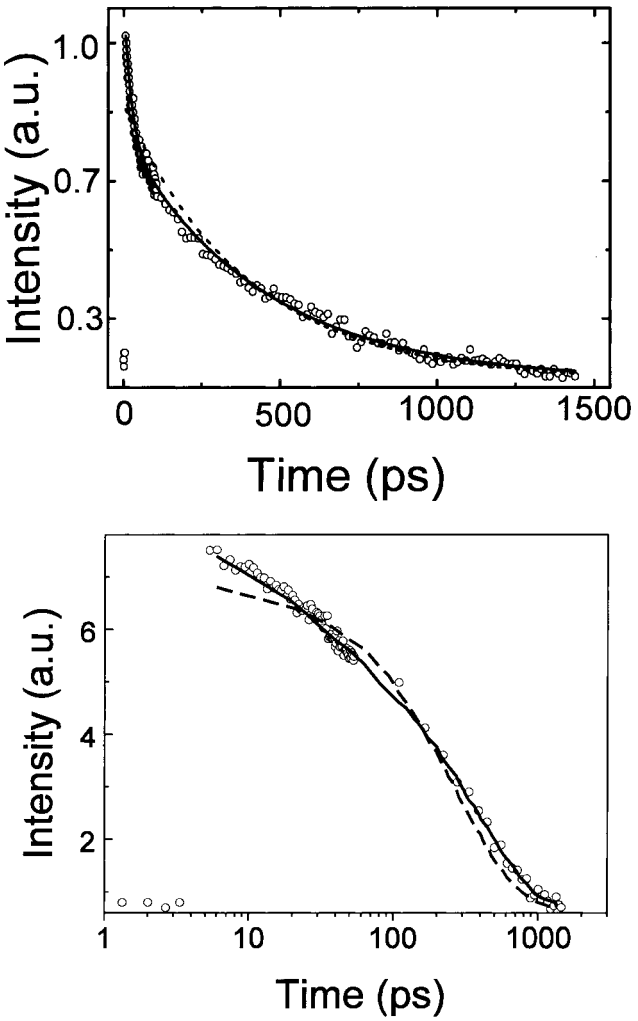

Figure 6. Plot of the anisotropy decays for ADC bound to **1**. Panel A (top) shows the observed decay law and panel B (bottom) is the same decay plotted on a logarithmic time axis. The dashed line is a best fit to a single exponential and the solid line is a best fit to a double exponential.

hydrodynamic model the effective relaxation time is 148 ps. In the slip model the relaxation times are the most different and range from 40 to 18 ps. Because the time constants differ by only a factor of 2 and they are similar in statistical weight, it is difficult to resolve the double exponential character of the decay law. The properly weighted average lifetime for the slip model gives a decay time of 29 ps which is in excellent agreement with the experimental value.

The important conclusion to draw from the free solute studies is that the relaxation is diffusive and the relaxation time is consistent with a slip boundary condition. This conclusion is consistent with earlier work on other solutes, which contain oxyanions,[5b,15] in DMSO. The relaxation times are also consistent with the values found for nonpolar anthracenes in DMSO solution (see Table 2). This result will allow constraints to be placed on the solute−solvent frictional coupling of the complexes, and hence the internal motion of the bound chromophore.

Orientational Relaxation of ADC Bound to 1 and 2. Figure 6 plots the measured orientational anisotropy for the ADC bound to the receptor **1**. In these data the host concentration was 10 times larger than the guest concentration. Two best fit curves to these data are shown in the figure. A single-exponential fit to the data is shown by the dashed line. Its

relaxation time corresponds to 350 ps. A double-exponential fit is shown by the solid line. The best fit parameters for the double-exponential form are 30% of a 26 ps component and 70% of 400 ps component. It is apparent from the plot that the double-exponential decay law provides much better agreement with the data. A comparison of the chi-square values for the two fits shows that the chi-square for the double exponential is 5 times smaller than that for the single exponential. Figure 6B shows the same data and fits as Figure 6A but the time axis is logarithmic. This method of presenting the data makes the deviations of the fitted curve from the measured data more apparent. This difference in the quality of the fits and the large time difference in the decay times found in the double-exponential fit provide convincing evidence that the decay is not a single exponential.

The similarity of the short time constant with that found for the unbound ADC in DMSO motivated a detailed study of the concentration dependence of the decay law. The anisotropy decay was measured at four different concentration ratios (1:3, 1:9, 1:13, and 1:17). For the case where the concentration ratio was 1:3, the anisotropy decay was fit by a double-exponential decay law with 27 ps (28%) and 216 ps (72%). Using this concentration ratio and the binding constants in Table 1, one expects about 1% of the ADC to be unbound. At the higher concentration ratios, the time constants were very similar to that reported in Table 1 and the relative amounts of the short and long time constants did not change over the range of concentration ratios. These data demonstrate that the signal's characteristics are not dependent on the concentration ratio of host to guest, as long as the host is present in reasonable excess. Hence the short time component of the anisotropy in Figure 6 reflects dynamics involving the ADC bound to the host.

The anisotropy decay of ADC bound to host **2** was also obtained with the host concentration present in large excess (1:10) for both data sets. The anisotropy decay of the ADC when it is bound in this host molecule is not exponential. A comparison of the fitting parameters to the anisotropy decays of the two systems shows that the fast time component for ADC in **2** is somewhat shorter than in **1**, but that the long time component is similar (see the data in Table 1). The short time constant obtained for the complex with **2** is 14 ps with a standard deviation of 4 ps, which is shorter than that found for the complex with **1**. The long time constant found for the anisotropy is similar for the two complexes. This similarity is consistent with the similarity in the overall size and shape expected for these two systems. In addition, the slow time constant is 10 times longer than that observed for the free ADC. These results support the identification of the longer time decay of anisotropy with the overall orientational relaxation of the complex, and the faster time, partial loss of anisotropy with an internal motion of the complex which occurs rapidly.

The assignment of the slow time constant to overall rotational relaxation is supported by a quantitative analysis. As with the rotational relaxation of the unbound chromophore molecules (vide supra), it is possible to characterize the time scale for the rotational relaxation of the complex by using the hydrodynamic model. A geometry for the complex of ADC with **1** was obtained by performing an ab initio calculation at the HF 3-21G level. Figure 7 provides a three-dimensional rendering of the complex. From this geometry one estimates the axial radii of the complex to be 8.3:8.3:2.8 Å. The volume was estimated to be 800 Å^3 from van der Waals increments. Using these geometric parameters, one computes a relaxation time of 590 ps for a stick boundary condition and 300 ps for a slip boundary

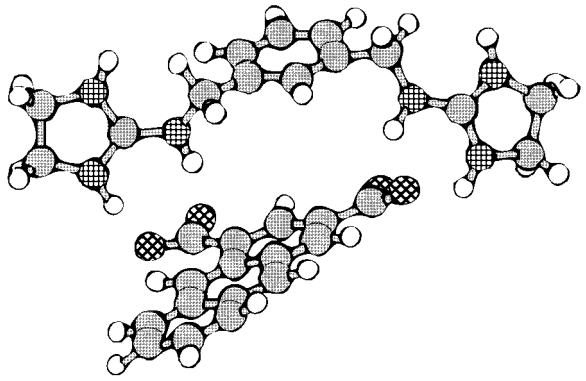

Figure 7. Computed geometry for the ADC:**1** complex. The open circles are hydrogen atoms, the shaded circles are carbon atoms, the rectangular hatched circles are nitrogen atoms, and the diamond hatched circles are oxygen atoms.

condition. It is clear that the long time constant measured has a magnitude similar to that expected for a rigid body whose size is similar to that of the entire complex.[13] The complex has a hydrodynamic boundary condition which is intermediate between the slip and stick limits. It has been established that as a rotating particle increases in size and roughness features relative to the solvent the boundary condition progresses toward the stick limit, even though it may be slip locally.[13b] In addition, a body of data indicates that cations rotating in DMSO solvent experience stronger frictional coupling than do anions.[5,14] The presence of local positive charges on the receptor would be expected to increase its drag with the solvent and hence change the effective hydrodynamic boundary condition. To conclude, the value of the long time decay of the anisotropy is consistent with that expected for the overall rotational relaxation of the complex.

The assignment of the fast anisotropy decay to internal motions of the chromophore in the complex is the most obvious based on the knowledge concerning the binding and the known mechanisms for the relaxation of the orientational anisotropy. Nevertheless, other possible mechanisms for the anisotropy decay were considered. Four possible sources for the fast anisotropy, other than internal torsional relaxation, were considered.

It is well-known that electronic energy transfer between chromophores can cause relaxation of the anisotropy.[18] The concentrations of the chromophore used here were $\sim 10^{-3}$ M, which indicates that this mechanism should not be active for the anthracene chromophore. Furthermore, the measurement of the anisotropy decay at concentrations ranging from 10^{-3} to 10^{-4} M for the solute in free solution showed no influence of concentration on the measured relaxation time.

A second mechanism for the decay of the anisotropy is by fast population relaxation of the excited electronic state. The fluorescence decay kinetics of the free chromophore and bound in the complex reveal that the effect of the excited state lifetime may be safely ignored. The excited state decay law of 1,3-ADC does not change significantly from the free molecule to that bound to the host molecules **1** and **2**. The decays have a mean fluorescence lifetime of 2.2−2.4 ns. In fact, the triplet yield for the anthracene may be considerable and since the OHPS method is probing ground state chromophores, the role of population kinetics is even less significant.[19] Another possible origin for the fast anisotropy could arise from a rotation of the transition dipole moment that is caused by a coupling between electronic states of the anthracene. This mechanism requires the presence of two low-lying electronic states, which

could be possible for this system.[19] To test this possibility, the anisotropy of the free solute was studied in DMSO and water/DMSO mixtures. The addition of water to the free ADC in DMSO causes a large increase in the fluorescence quantum yield, similar to that found for binding of the ADC with **1** and **2**. Presumably, this increase in the fluorescence arises from complexation of the water with the carboxylate, and it provides a method to mimic the local environment around the chromophore in the complex. The anisotropy decay of the free solute becomes longer as water is added to the DMSO solution. No occurrence of a nonexponential decay law or a shortening of the anisotropy is found. These data indicate that if interstate dynamics is occurring in these systems it is not modifying the anisotropy in the way found for the complexes. The observation of a longer anisotropy decay supports the hypothesis that the water hydrogen bonds to the carboxylate, increasing its "hydrodynamic volume" and hence its rotational relaxation time.[15,16]

Lastly, it was considered that the fast component might arise from a rigidly bound ADC chromophore but highly anisotropic motion of the complex. For an oblate rotor of the type in Figure 7 with the transition dipole moment located in the plane of the rotor, the anisotropy decay law is predicted to be

$$r(t) = \frac{2}{5}\left[\frac{1}{4}\exp(-6D_{\perp}t) + \frac{3}{4}\exp(-(4D_{\parallel} + 2D_{\perp})t)\right] \quad (2)$$

where $D_{\perp}$is the diffusion constant for out-of-plane motion and $D_{\parallel}$ is the diffusion constant for the in-plane motion. Evaluation of these diffusion constants using slip hydrodynamics results in anisotropy relaxation times for the complex that are significantly longer than that observed—100 ps and longer. In fact, the fast relaxation time of 16 ps observed for the complex with **2** is only 4 times slower than the mean rotational period τ_{FR} of the molecule, where $\tau_{FR} = (2\pi/9)(kT/I)^{1/2}$ and I is the inertial moment. Free rotation or nearly free rotation of a molecule this size and shape in solution would be unprecedented. In fact, it is significantly more likely that such a behavior be displayed by 9,10-disubstituted anthracenes, based on their size and shape, and it is certainly not observed for those systems.

Given the assignment of the fast relaxation to the relative internal motion of the chromophore with respect to the host molecule, an important qualitative feature of the anisotropy's relaxation is the monotonic decay rather than a decay with oscillations. If the motion were underdamped, then the anisotropy decay would appear as a damped sinusoid rather than the simpler form observed here.[20] The type of decay law presented in Figure 6 is expected for an overdamped oscillator. This observation is consistent with the open (solvent accessible) nature of the binding site in these compounds, in which the frictional coupling with the solvent can be high. During the time period of its orientational motion (presumed to be a low-frequency bend), the guest chromophore experiences a large number of collisions with solvent molecules. Hence the relaxation appears to be diffusional.

V. Models

In order to better characterize the fast dynamics, one must employ a model. Three types of modeling were pursued in order to see if the fast relaxation observed here is consistent with physical expectations for the torsional motion of the ADC moiety. First, two analytical models for the relaxation were considered: diffusion over a restricted angular range and diffusion in a harmonic potential. The third model used was a molecular dynamics simulation of the complex with **1**.

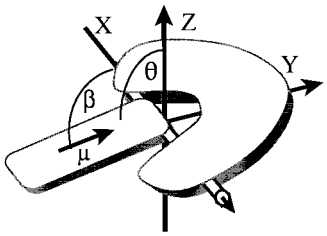

Figure 8. Essential geometry and axis system used to describe the internal motion of the chromophore. The chromophore diffuses about the *X* axis which is defined by the interaction sites between the carboxylates and the guanidiniums. The angle between the transition dipole moment and the *X* axis in the X−Y plane is given by β. The angle θ defines the orientation of the transition dipole moment with respect to the *Z* axis in the molecular frame.

An ab initio calculation at the HF 3-21G level was used to obtain a realistic geometry for the ADC:**1** system. The geometry obtained for the complex is shown in Figure 7. The axis of internal torsion for the complex is defined by the "point contacts" of the carboxylates on the ADC with the guanidinium moieties of the host. A CIS calculation was performed at the equilibrium geometry to determine an appropriate transition moment direction for the chromophore. The transition moment for ADC lies in the plane of the molecule and subtends an angle of 68° with the long axis of the anthracene chromophore. It is rotated toward the 1-position of the anthracene ring. This geometry places the transition dipole at an angle of 34° with respect to the axis of internal rotation.

One approach to the treatment of internal motion is to treat it as diffusion over a restricted angular range, usually approximated as a cone defined by the angle θ of its apex.[20−22] In this case the amount of the anisotropy loss which results from the fast decay can be used to estimate the angle of the cone. Wahl considered the one-dimensional cone model. In this model the chromophore diffuses about an axis in which the rotation is limited to an angular range of $-\theta_{max}$ to θ_{max} (see Figure 8), and the conical surfaces act as reflecting boundaries in the solution of the diffusion equation. For the system studied here the rotation axis would be defined by the axis connecting the two point interaction sites. More elaborate models could be exploited which allow the axis to also wobble.[20]

This model gives an expression for the anisotropy decay $r(t)$ which is an infinite sum of exponentials. By considering the anisotropy for the diffusion in the cone to be much faster than the overall rotational diffusion of the entire complex, an intermediate time scale τ_{int} can be identified. This time scale corresponds to total relaxation of the anisotropy resulting from the internal motion but no relaxation arising from the overall diffusion; i.e., slower motion. In this case one can evaluate Wahl's expression[21] for $r(\tau_{int})$. If the transition dipole is taken to lie in the plane of the complex one finds

$$\frac{r(\tau_{int})}{r(t=0)} = [P_2(\cos^2\beta)]^2 + \frac{3}{4}\sin^4\beta\,\frac{\sin^2(2\theta_{max})}{(2\theta_{max})^2} + \frac{3}{4}\sin^2 2\beta\,\frac{\sin^2\theta_{max}}{\theta_{max}^2} \quad (3)$$

for the long time behavior of the anisotropy, where β is the angle between the transition dipole and the axis of internal rotation. Using a value of 34° for β and the amplitude of the long component lifetime for the ratio in eq 3, one finds a θ_{max} of 60° for the chromophore bound with **1** and 40° for the chromophore bound with **2**.

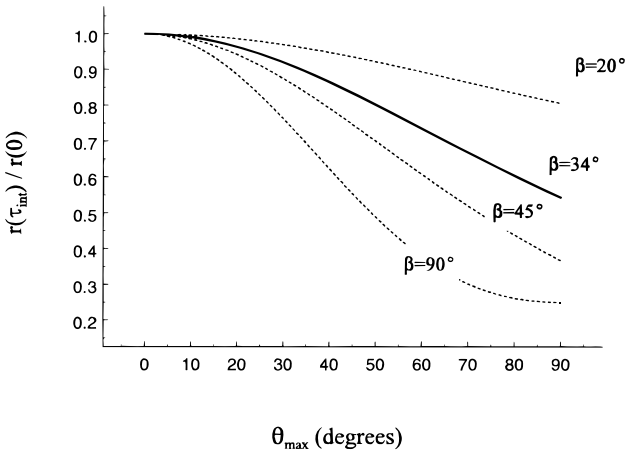

Figure 9. Ratio predicted by the Wahl model for diffusion about a fixed axis as a function of the transition dipole moment orientation with respect to the torsion axis (β) and the maximum angular deviation (θ_{max}). The solid curve corresponds to $\beta = 34°$ which is calculated for the ADC complex with **1**.

Figure 9 illustrates how the ratio in eq 3 depends on the parameters θ_{max} and β. Given that the separation of time scales is reasonable, the ratio in eq 3 represents the amplitude of the long component lifetime in the fit to a double exponential. Figure 9 plots the amplitude of the long component versus the angular deviation θ_{max} for four different values of the angle β. These plots demonstrate that an accurate determination of the transition dipole moment direction with respect to the torsional axis is necessary for making reasonable estimates of the angular deviation of the chromophore. For example, when β is 90°, one finds a θ_{max} value of 32° for ADC with **1** and a θ_{max} value of 25° for ADC with **2**. These values are significantly different than those found for a β value of 34° reported above. In fact, the choice of $\beta = 90°$ most severely restricts the value of θ_{max}. It is apparent that the chromophore in this system has a range of motion which is ±25° or larger. This result is consistent with the open structure of this complex.

A more realistic modeling of the complex's internal motion should account for the presence of a potential. Szabo[20] has developed a more sophisticated treatment of the relaxation of a chromophore that is bound to a macromolecule, and he finds an expression for the anisotropy decay. In this model the intermolecular potential between the chromophore and the macromolecule is treated as harmonic. The adequacy of such an approximation for such a low-frequency motion is open to question; nevertheless, it provides a starting point for a discussion of the dynamics and provides an avenue to assess the reasonableness of the potential parameters. The approximation used here is to assume that the overall rotational relaxation of the complex can be described by a single relaxation time τ_{cmplx}. In general, for a system with the oblate shape expected for the complex one expects the anisotropy to be a sum of two decaying exponentials such as that given in eq 2. However, the decay times for the two exponentials are very similar (266 and 307 ps for the case of a slip boundary condition) and cannot be resolved experimentally. Hence it is reasonable to approximate the relaxation as a single-exponential decay whose decay time is the properly weighted sum of the decay times for the two terms in the anisotropy formula.

With the two approximations that the overall rotational relaxation of the complex is isotropic and the axis for internal rotation is fixed in the molecular frame, one can use eq 4.5 of reference 9 to write

$$r(t) = \frac{2}{5}\exp(-t/\tau_{cmplx})\left[[P_2(\cos\beta)]^2 + \frac{3}{4}\sin^2 2\beta\,\Gamma_{11}(t) + \frac{3}{4}\sin^4\beta\,\Gamma_{22}(t)\right] \quad (4)$$

where $P_2(x)$ is the second Legendre polynomial and β is the polar angle between the rotation axis and the transition dipole of the chromophore. The geometry found in Figure 7 for ADC with **1** places the transition dipole at an angle β of 34°. A comparison of this expression with eq 3 obtained from Wahl's treatment demonstrates that the geometric factors are the same. The difference between the two treatments lies with the model for the relaxation given by the angular time-correlation functions $\Gamma_{nn}(t)$.

The modeling of the form of the relaxation remains. Szabo[20] considered both inertial and diffusive relaxation of the chromophore in a harmonic potential. For the case of inertial dynamics he found an expression for $\Gamma_{nn}(t)$ which is oscillatory (eq 6.10a of ref 20). The decay observed for ADC bound in the complexes studied here does not show oscillations. For this reason, only the diffusive relaxation is considered. In this limit, Szabo obtained

$$\Gamma_{11}(t) = \exp\left[-\frac{kT}{I\omega^2}\left[1 - \exp\left(-\frac{\omega^2 IDt}{kT}\right)\right]\right] \quad (5)$$

and

$$\Gamma_{22}(t) = \exp\left[-\frac{4kT}{I\omega^2}\left[1 - \exp\left(-\frac{\omega^2 IDt}{kT}\right)\right]\right] \quad (6)$$

for the angular correlation function, where I is the reduced moment of inertia and ω is the frequency of the intermolecular host−guest potential. This frequency is characteristic of the relative internal motion of the host and guest. The goal of this analysis is to provide an estimate of this frequency for the ADC:**1** and ADC:**2** systems. The diffusion coefficient is connected to the friction through the Einstein relation ($D = kT/\zeta$).

Combining eqs 4−6, the harmonic well frequency and diffusion constants can be obtained from a best fit to the experimental data. The data were fit to this form using $\beta = 34°$. The fit includes three primary parameters which correspond to the overall relaxation time of the complex τ_{cmplx}, the diffusion coefficient of the anthracene in the potential D, and the frequency of the potential ω. A best fit of this form is shown in Figure 10 for the case of the complex with **2** in DMSO at 303 K. The data are plotted versus a logarithmic time axis so that the quality of the fits can be compared over the large time range. The parameters obtained from a fit of this model to the measured anisotropy decays are summarized in Table 3.

Three features of these parameters are noteworthy. First, the diffusion constant D is similar for the two complexes. This diffusion constant should depend on the interaction between the guest chromophore and the solvent. In the context of the model, the diffusion coefficient D is an effective diffusion constant for the internal motion and does not strictly correspond to the diffusion constant of the guest chromophore. Nevertheless, a very good correspondence exists between this value and the diffusion constants that are measured for nonpolar anthracenes in DMSO. This observation is consistent with the carboxylate moiety localized in the binding site and the nonpolar part of the molecule exposed to the solvent. Second, the relaxation

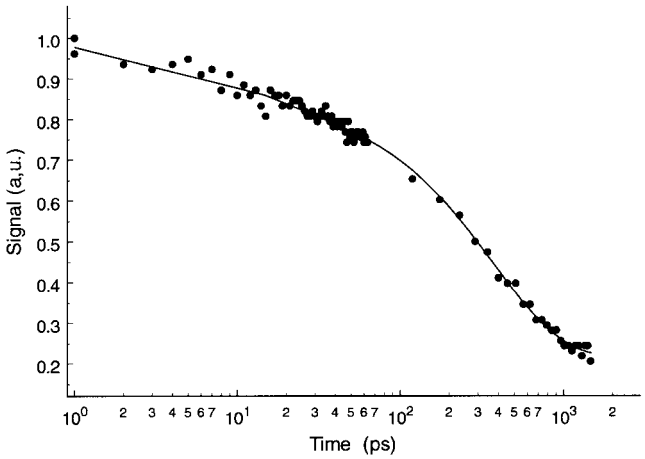

Figure 10. Experimental decay curve for the complex with **2** in DMSO at 303 K. The line represents a best fit of the data to eq 4.

TABLE 3: Diffusion Constants, Frequencies and Angular Displacements for the Two Host−Guest Systems

	complex with **1**	complex with **2**
D, ns^{-1}	18	14
D_{cmplx}, ns^{-1}	0.45	0.46
ω,[a] cm^{-1}	27	32
θ_{max},[b] deg	60	40

[a] The frequency is estimated using an inertial moment of 2.1×10^{-44} kg m^2, which was obtained from the optimized geometry of the complex. [b] The angle is obtained by using a model for diffusion in a cone and assuming that $r(0)$ is exactly 0.4.

time obtained for the overall diffusion of the complex is similar for the two complexes. Because the complexes have a similar size and shape, their overall rotational diffusion should be similar. It is possible to estimate the diffusion constant expected for the overall rotation using a hydrodynamic model, and the value obtained from the fit lies between the two extremes of stick and slip hydrodynamics (vide supra). Third, the characteristic well frequency of the complex with **2** appears to be slightly larger than that of the complex with **1**, but this difference is too small to interpret safely. The diffusion coefficients and frequencies extracted from the data are reasonable on a physical level.

It is possible to use these two models, diffusion in a one-dimensional cone and diffusion in a harmonic potential, to determine the root mean square angular displacement for the chromophore. In the Wahl model the chromophore diffuses over a range of angles from $-\theta_{max}$ to θ_{max}, so that the average angle is given by 0° and the root mean square angle is $\theta_{rms} = (\theta_{max}/3)^{1/2}$. Using the θ_{max} values in Table 3 one finds $\theta_{rms} =$ 35° for the complex with **1** and $\theta_{rms} = 23°$ for the complex with **2**. For the case of the harmonic potential, the average angular displacement is zero and the mean square angular displacement is given by $\theta_{rms} = (kT/I\omega^2)^{1/2}$. Using the frequencies and inertial moment reported in Table 3, one finds $\theta_{rms} =$ 33° for the complex with **1** and $\theta_{rms} = 27°$ for the complex with **2**. The agreement in the θ_{rms} for these two different models is quite good. This good agreement supports the conclusion that the motion for this system may be treated as diffusion in a constrained geometry.

Lastly, a molecular dynamics trajectory was performed for the complex (in vacuo) in order to test whether the nature of the motion and its frequency is consistent with the modeling provided above. The molecular dynamics trajectory for the complex of ADC with **1** was run using the Discovery Model of the Insight II software package (MSI). The CVF89 force field was used and the temperature was set to 300 K. The equilibrium geometry used for the complex was that found from a Hartree−Fock calculation. The trajectory was begun with the complex in its equilibrium geometry and was allowed to proceed for 100 ps. Figure 11 shows a plot of the $\cos^2\theta$ as a function of time. The period of the motion is found to be a few picoseconds and corresponds to a frequency of 2.5×10^{11} Hz (9 cm^{-1}). This value is smaller than that obtained from an analysis of the data using the Szabo model but is consistent with it. The mean square angular displacement can also be obtained from this trajectory and one finds a value of ±28°. This angular fluctuation is also consistent with the open architecture of this intermolecular complex.

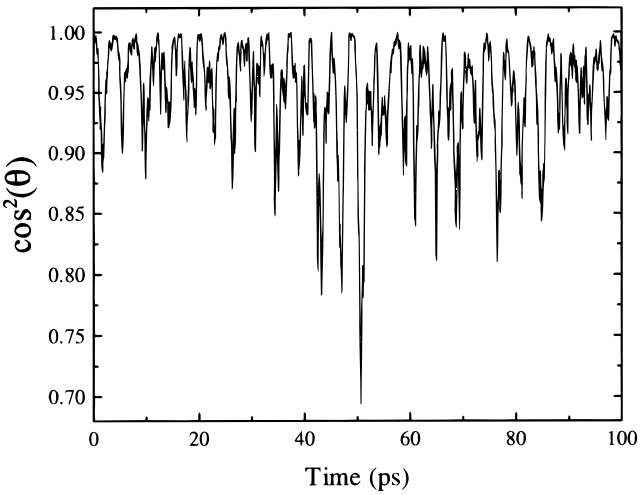

Figure 11. Plot of the function $\langle \cos^2\theta(t) \rangle$ versus time.

These three approaches to modeling the internal dynamics of the chromophore provide a consistent view of the complex's flexibility. The analysis suggests a large-amplitude motion for the chromophore, of the order of 30−40° (in the case of ADC: **2**), with a frequency that is consistent with a librational or torsional mode (30 cm^{-1}). These two parameters (range of the motion and the frequency) are corroborated by the preliminary MD results for the complex's motion. A more detailed MD study in which solvent will be included is underway.

VI. Conclusions

In conclusion, the relative motion of the bound host−guest complexes was studied using the time-resolved polarization spectroscopy method. The orientational relaxation of the ADC bound to **1** and **2** shows a rapid initial relaxation that is followed by a much slower relaxation. This result is contrasted with a single-exponential relaxation for the free ADC molecule in solution. By changing the geometry of the host molecule, the host−guest interaction and the observed relaxation dynamics were changed. A damped oscillator model can be used to fit the data and estimate the frequency of the host−guest potential. The values obtained for the frequency are consistent with those expected for a low-frequency bending motion. From the diffusion in a cone model the range of guest angular motion was obtained. The experimental decays showed no oscillatory behavior, indicating that the relaxation is diffusive. Future studies will explore these issues further.

Acknowledgment. This work is supported by grants from the National Science Foundation (CHE-9416913 to D.H.W., and CHE921937 to A.D.H.). The authors thank Andrew Carr and

Maria and Igor Kurnikov for the valuable discussions and support. We thank Prof. P. Wipf for advice on the synthesis of the guest chromophore.

References and Notes

(1) Jardetzky, O. *Prog. Biophys. Mol. Biol.* **1996**, *65*, 171.

(2) Lakowicz, J. R. *Proceedings of the SPIE 1204*; SPIE: Bellingham WA, 1990.

(3) (a) Schiessl, P.; Schmidtchen, F. P. *Tetrahedron Lett.* **1993**, *34*, 2449. (b) Müller, G.; Riede, J.; Schmidtchen, F. P. *Angew. Chem.* **1988**, *27*, 1516. (c) Echavarren, A.; Galán, A.; Lehn, J. M.; Mendoza, J. *J. Am. Chem. Soc.* **1989**, *111*, 4994.

(4) (a) Dixon, R. P.; Geib, S. J.; Hamilton, A. D. *J. Am. Chem. Soc.* **1992,** *114*, 365. (b) Jubian, V.; Dixon, R. P.; Hamilton, A. D. *J. Am. Chem. Soc.* **1992**, *114*, 1120. (c) Linton, B. Ph.D. Thesis, University of Pittsburgh, 1997.

(5) (a) Alavi, D. S.; Hartman, R. S.; Waldeck, D. H. *J. Chem. Phys.* **1989**, *92*, 4055. (b) Alavi, D. S.; Hartman, R. S.; Waldeck, D. H. *J. Chem. Phys.* **1991,** *94*, 4509.

(6) Cerullo, G.; De Silvestri, S.; Magni, V. *Opt. Lett.* **1994**, *19*, 1040.

(7) Leon, J. W.; Whitten, D. G. *J. Am. Chem. Soc.* **1995**, *117*, 2226.

(8) Hallman, J. L.; Bartsch, R. A. *J. Org. Chem.* **1991**, *56*, 6243.

(9) Dey, J.; Haynes III, J. L.; Warner, I.; Chandra, A. K. *J. Phys. Chem. A* **1997**, *101*, 2271. Werner, T. C.; Hercules, D. M. *J. Phys. Chem.* **1970**, *74*, 1030.

(10) Cowan, D. O.; Schmiegel, W. W. *J. Am. Chem. Soc.* **1972**, *94*, 6779. Suzuki, S.; Fujii, T.; Yamanaka, S.; Yoshiike, N.; Hayashi, Z. *Bull. Chem. Soc. Jpn.* **1979**, *52*, 742.

(11) Wiseman, T.; Williston, S.; Brandts, J. F.; Lin, L. N. *Anal. Biochem.* **1989**, *179*, 131.

(12) Hartman, R. S.; Konitsky, W. M.; Waldeck, D. H.; Chang, Y. J.; Castner Jr., E. W. *J. Chem. Phys.* **1997**, *106*, 7920.

(13) (a) Fleming, G. R. *Chemical Applications of Ultrafast Spectroscopy*; Oxford: New York, 1986. (b) Williams, a. M.; Jiang, Y.; Ben-Amotz, D. *Chem. Phys.* **1994**, *180*, 119.

(14) (a) Hartman, R. S.; Alavi, D. S.; Waldeck, D. H. *Isr. J. Chem.* **1993**, *33*, 157. (b) Balabai, N.; Sukharevsky, A.; Read, I.; Strazisar, B.; Kurnikova, M.; Hartman, R. S.; Coalson, R. D.; Waldeck, D. H. *J. Mol. Liq.*, accepted.

(15) (a) Fleming, G. R., Morris, J. M.; Robinson, G. W., *Chem. Phys.* **1976**, *17*, 91. (b) Spears, K. G.; Steinmetz, K. M. *J. Phys. Chem.* **1985**, *89*, 3623.

(16) Zwanzig, R.; Harrison, A. K. *J. Chem. Phys.* **1985**, *83*, 5861.

(17) Bondi, A. *J. Phys. Chem.* **1964**, *68*, 441.

(18) Lakowicz, J. R. *Principles of Fluorescence Spectroscopy*; Plenum: New York, 1983.

(19) Cross, A. J.; Waldeck, D. H.; Fleming, G. R. *J. Chem. Phys.* **1983**, *78*, 6455.

(20) Szabo, A. *J. Chem. Phys.* **1984**, *81*, 150.

(21) Wahl, P. *Chem. Phys.* **1975**, *7*, 210.

(22) (a) Schurr, J. M. *Chem. Phys.* **1982**, *65*, 417. (b) Fisz, J. J. *Chem. Phys.* **1994**, *181*, 425. (c) Lipari, G.; Szabo, A. *J. Chem. Phys.* **1981**, *75*, 2971.